IEEE Access
Multidisciplinary ⋮ Rapid Review ⋮ Open Access Journal

Received January 9, 2019, accepted January 17, 2019, date of publication January 31, 2019, date of current version February 22, 2019.

Digital Object Identifier 10.1109/ACCESS.2019.2896598

Realizing Multi-Gbps Vehicular Communication: Design, Implementation, and Validation

GOSAN NOH, (Member, IEEE), JUNHYEONG KIM, HEESANG CHUNG, AND ILGYU KIM
Electronics and Telecommunications Research Institute, Daejeon 34129, South Korea

Corresponding author: Gosan Noh (gsnoh@etri.re.kr)

This work was supported by Institute of Information and communications Technology Planning and Evaluation (IITP) grant funded by the Korean Government (MSIT) (No. 2018-0-00792, QoE improvement of open Wi-Fi on public transportation for the reduction of communication expense).

ABSTRACT This paper proposes a vehicular communication system that can achieve multi-Gbps data rate transmission for train and car applications. Employing a millimeter-wave frequency band around 25 GHz, the proposed system provides mobile backhaul connectivity for vehicle user equipments (UEs). In order to support a very high data rate with such a high carrier frequency while guaranteeing sufficient robustness against high mobility-related behaviors such as fast channel variation and unstable handover, we employ a relaying network architecture consisting of a backhaul link to a vehicle UE and an in-vehicle access link. Based on that, we provide a set of fundamental design elements including numerology, frame structure, the reference signal, multi-antenna scheme, and handover. We then validate the proposed vehicular communication system by implementing an experimental testbed consisting of baseband modem, RF front end, an array antenna units, and by performing field trials in an actual subway tunnel and urban road environments. The experimental validation results reveal that providing multi-Gbps backhaul transmission is possible and worthwhile for both train and car scenarios.

INDEX TERMS 5G, high mobility, mmWave, testbed, vehicular communications.

I. INTRODUCTION

The fifth generation (5G) wireless systems aim to provide highly ambitious goals, namely multi-Gbps data rate, near-100% reliability, and sub-ms latency, each of which can be matched to the three main 5G use cases of enhanced Mobile BroadBand (eMBB), Ultra-Reliable Low-Latency Communication (URLLC), and massive Machine-type Communication (mMTC) [1]. These 5G requirements are to be fulfilled in various deployment scenarios, among which vehicular communication scenarios for providing wireless connectivity to trains and cars have attracted great attentions from both research and industry communities [2], [3].

Such vehicular deployment scenarios are characterized by the high mobility, e.g., speeds of 140 km/h for cars driving on highways [4] and 500 km/h for high speed trains [5]. These high mobility requirements for vehicular scenarios greatly affect the system design and implementation, which will be quite different from the traditional cellular environments optimized to low-to-mid mobility scenarios. Due to such highly mobile nature of the vehicular scenarios, there arise several technical challenges to be overcome, particularly in fast channel variations due to large Doppler shift/spread and unstable handover operations [2].

Another important consideration is the use of millimeter wave (mmWave). In order to achieve the above-mentioned multi-Gbps data rate, it is necessary to have a frequency band as wide as a few GHz, which is not generally obtainable in conventional below-6 GHz frequency bands. A wide bandwidth of over a few GHz is indeed available in the mmWave bands, but it also comes with additional challenges. Since the Doppler shift/spread is proportional to the carrier frequency, the above-mentioned Doppler-induced problems become further severe [6]. In addition, mmWave signals not only experience high free space path loss from Friis law, but also suffer from additional losses due to poor diffraction, rain attenuation, atmospheric absorption, and high penetration loss [7], [8].

Considering the above aspects of high mobility and mmWave frequency bands, the objective of this paper is to find the best design and implementation solutions that can realize multi-Gbps vehicular communication.

The associate editor coordinating the review of this manuscript and approving it for publication was Min Li.

A. RELATED WORK

We first survey the existing already deployed high mobility communication systems including railway and vehicle-to-everything (V2X) communication systems. Global System for Mobile communication (GSM) was extended to a railway-specific version called GSM-R, which can support voice and data communications for railway operations. The maximum data rate of GSM-R is 172 kbps [9]. Mobile WiMAX is based on IEEE 802.16 technology and enables mobile communication with the maximum supported throughput of a few hundred Mbps. The Mobile WiMAX system was used to provide wireless backhaul connectivity for the onboard WiFi service of Seoul subway system in Korea, with the average data rate on the order of 10 Mbps. Long Term Evolution (LTE) was extended to LTE-R, which was introduced to overcome the limitations of GSM-R and to cope with the new railway services such as real-time monitoring, multi-media dispatching, and railway internet-of-things (IoT) [9]. The maximum data rate of LTE-R is around 50 Mbps in the downlink and 10 Mbps in the uplink, respectively [9]. IEEE 802.11p-based dedicated short-range communication (DSRC) targets safety-related V2X services. The DSRC operates in a distributed manner, namely carrier-sense multiple access (CSMA), thereby potentially experiencing performance degradation due to, for example, a hidden node problem [10]. The data rate of the DSRC system is on the order of 10 Mbps. LTE V2X can fully utilize existing LTE infrastructure and can improve V2X efficiency. The LTE V2X standardization has been completed in 2017 with Release 14 and is expected to be deployed in near future [10]. The LTE V2X can achieve the data rate on the order of 100 MHz.

There is a lot of existing work on mmWave-based high mobility transmission in several aspects such as network architecture, channel characterization and modeling, numerology and frame design, channel estimation, time/frequency offset compensation, multi-antenna scheme, handover, and so on.

A relay-based network architecture for vehicular communication systems especially for high speed train has been widely investigated [11]–[13]. By deploying mobile onboard relays, Internet connectivity can be better provided to the train passengers. A relay-based dual-link handover scheme was proposed based on the cooperation between front and rear antennas in [11]. A mobile relaying scheme was employed in LTE Advanced (LTE-A)-based high speed rail networks, which can reduce handover overheads [12]. In [13], a mobile relay architecture was investigated in the aspects of high speed train channel modeling.

Temporal channel variation characteristics of the mmWave-based vehicular system were investigated in [14], where the impact of beamwidth was analyzed using the concept of beam coherence time. Channel models for high speed train moving at a speed up to 500 km/h were developed for various railway environments using 3D ray tracing simulations [15], [16]. Ray tracing-based channel modeling was also conducted for the mmWave-based V2X communications, showing the effects of beam alignment and beamwidth [17]. Channel measurements focusing on path-loss were conducted at 28 GHz for vehicle-to-vehicle (V2V) communications [18]. V2V channel measurements were also provided focusing on impulse response, scattering function, Doppler spread, and delay spread at 38 GHz and 60 GHz frequency bands [19]. In [20], the effects of the obstacles on the V2V and vehicle-to-infrastructure (V2I) scenarios were investigated from the measurements and ray-tracing simulations.

Investigations on numerology and frame structure for high mobility systems were provided in several existing works. Subcarrier spacing and rate adaptation schemes were proposed for supporting very high mobility scenarios [21]. Several design elements including numerology and frame structure for the 3GPP 5G New Radio (NR) specifically targeting high speed train scenario were provided in [22]. A feasible frame structure for mmWave-based high speed railway communications was investigated in [23].

Improved channel estimation techniques are needed to cope with the highly time-selective nature of the mmWave-based high mobility applications. A study on the time-domain pilot density optimization was done for maximizing the spectral efficiency in high mobility systems [24]. The design and evaluation of demodulation reference signal (DMRS) for supporting 5G NR high speed train scenario were provided in [25], where the DMRS pattern with high time-domain and low frequency-domain densities was shown to be highly beneficial. An adaptive channel estimation technique was proposed for vehicular applications [26], where location information was used to reduce channel estimation time and to improve channel estimation accuracy.

The effect of frequency offset is more significant when the carrier frequency becomes higher on top of the very high mobility. In this regard, new Doppler shift estimation schemes were proposed for mmWave communication systems on high speed railway [27]. A frequency offset compensation scheme was proposed in [28], where both the pre-compensation at the transmitter and the post-compensation at the receiver were utilized.

Regarding the multi-antenna scheme for mmWave high mobility systems, beamforming and massive multiple-input-multiple-output (MIMO) techniques have been studied. In [29], a hybrid spatial modulation beamforming scheme was proposed which can be used for high speed railway systems operating at a mmWave frequency band. For intelligent transportation systems (ITS) applications, a motion prediction-based beam steering algorithm was proposed which exploited beacon information broadcasted by vehicles [30].

In principle, mmWave-based high mobility communication systems intrinsically experience handover performance degradation due to, for example, very frequent handover and blockage. A robust handover scheme based on dual connectivity was proposed in [31], where both the 4G and 5G

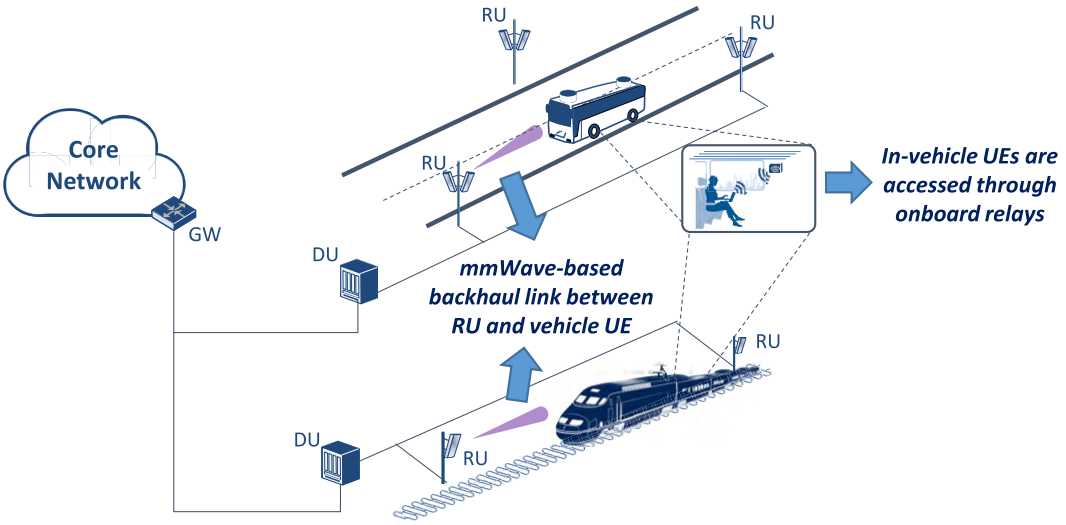

FIGURE 1. Relaying network architecture for vehicular communications: Bus scenario (top) and train scenario (bottom).

networks can be simultaneously connected. A handover interruption time reduction scheme was proposed, which relies on the dual-layer and dual-link architecture and the coordination of front and rear antennas of a train [11]. The use of distributed antenna system (DAS) was proposed in order to tackle the frequent handover problem, where distributed antennas connected to a central unit through radio-over-fiber (RoF) were used to transmit the same signal to a UE, thereby transforming handover procedure into an antenna selection procedure [32]–[34]. Coordinated multi-point (CoMP) technology can also be used to enable uninterrupted handovers for a UE by combining signals from multiple base stations [35].

Standardization efforts have been conducted on the mmWave-based high mobility use cases such as high speed train and V2X scenarios in the 3GPP 5G NR specification. In [36], several 5G NR high speed train communication standardization issues were discussed including network architecture, initial access, mobility management, and physical layer design. Different from the LTE V2X which is limited to the legacy below-6 GHz band, NR V2X additionally introduced the mmWave band for its V2I and V2V links [4]. The overview of the 5G V2X physical layer design can be seen in [37].

It should be noted that the 5G NR system intrinsically needs to satisfy diverse requirements in many aspects such as the carrier frequency from hundreds of MHz to nearly 100 GHz, the coverage range from tens of meters to hundreds of kilometers, the mobility from 0 to 500 km/h, the connection density up to $1,000,000$ devices/km^2, and so on. However, for doing that, the 5G NR system requires large control overhead and complex protocol procedures.

B. CONTRIBUTIONS AND ORGANIZATION

With the purpose of satisfying the high mobility-related 5G requirements, in this paper, we propose a vehicular communication system which is particularly well suited for the mmWave frequency bands in the high mobility scenarios, thereby enabling a light-weight design which can potentially minimize the control overhead and implementation complexity. In this regard, we provide a collection of network architecture, system design, testbed implementation, and experimental validation for realizing multi-Gbps vehicular communication with special emphases on train and car applications. More specifically, as a continuation of our previous works [38], [39], we present a relaying network architecture where each user equipment (UE) inside a vehicle is accessed through an onboard relay. Deployed on a train or a car, the onboard relay can establish backhaul connectivity to the network, which is more efficient and reliable than the direct access of the in-vehicle UEs to the network. We then describe the details of the system design including numerology, frame structure, reference signal, multi-antenna scheme, and handover, all of which are specifically tailored for the high mobility operations. Based on the proposed system design, we present our testbed implementation consisting of baseband modem, RF front-end, and antenna. We finally validate the testbed through the real-world field tests in subway tunnel and urban road environments.

This paper is organized as follows. Section II describes the proposed vehicular communication system. The design elements of the proposed system are presented in Section III. Section IV delivers testbed implementation and validation aspects, and Section V concludes the paper.

II. SYSTEM DESCRIPTION

The main focus of the proposed vehicular communication system is to provide multi-Gbps wireless connectivity to vehicle UEs such as trains and buses, as seen in Fig. 1. The base station functionalities are distributed between a data unit (DU) (also called baseband unit (BBU)) and a radio unit (RU) (also called radio remote head (RRH)). Each DU is mainly responsible for baseband and higher layer

processing, and is connected to the core network through a gateway (GW). Each RU performs up/down-conversion between baseband and RF signals and transmission/reception of RF signals through antennas. Several RUs are deployed along the road or railway tracks and are connected to a DU. The interconnection between the DU and RU is through radio-over-fiber (RoF) links, which is a cost-effective and flexible solution [40], [41].

The in-vehicle UEs inside a train or a bus can access the network through an onboard relay deployed on such transportation vehicles. The onboard relay is provided with wireless connectivity to the network through a backhaul link between the RU and a vehicle. Inside the vehicle, we can employ existing WiFi or femto cell technology, where the propagation environment is quite similar to indoor scenario. This relaying network architecture has several advantages over the direct access that connects in-vehicle UEs directly to the network infrastructure such as RUs. First, by relaying signals through the onboard relay, it is possible to avoid severe signal penetration loss due to a metallic vehicle body, which can be up to 20-35 dB [2]. Second, the relaying architecture is also advantageous to avoid the problem of so-called signaling storm due to group handover, which arises in a situation when a lot of UEs (there may be hundreds of active UEs in a train) cross the cell boundary and try to perform handover at the same time, thereby leading to network congestion and handover failure [2], [42].

We employ the mmWave frequency band around 25 GHz for the backhaul links between the RUs and vehicle UEs, thus enabling a large bandwidth on the order of GHz. This large bandwidth is a prerequisite for providing multi-Gbps backhaul connectivity which needs to support tens to hundreds of in-vehicle UEs inside the buses and trains. It is known that mmWave frequency bands may suffer from higher propagation loss [7], [8]. However, thanks to its short wavelength properties, high-gain directional beamforming can be easily implemented so as to generate quite narrow beams. This beamforming technique can confine and concentrate the beams into the road and railway areas, minimizing potential interference to other nearby devices as well as increasing coverage. In addition, there will be usually no or few blocking obstacles on the roads (especially on highways) and train tracks, provided that the RUs are properly installed.

III. SYSTEM DESIGN ELEMENTS

This section describes essential system design elements for the proposed vehicular communication system. We first focus on the physical layer baseband processing structure, which is specifically designed to be highly Doppler tolerant. We then propose a handover enhancement scheme with a focus on vehicle applications.

A. DOPPLER-TOLERANT PHYSICAL LAYER STRUCTURE

In the proposed vehicular communication system, an orthogonal frequency-division multiple access (OFDMA) transmission scheme is employed both for the downlink and uplink. Considering a relatively alleviated peak-to-average power ratio (PAPR) requirement for the vehicle UEs having loosened power and size constraints, a single-carrier frequency-division multiple access (SC-FDMA) scheme, which is based on discrete Fourier transform-spread-OFDM (DFT-s-OFDM) waveform, is not employed in the uplink. As a duplex scheme, time-division duplex (TDD) is used, which has better adaptability to the asymmetric and varying traffic ratio between the downlink and uplink. In addition, the TDD scheme has less complexity especially for mmWave RF circuitry [43].

The OFDM numerology design is involved not only in the mmWave channel characteristics but also in the highly mobile nature of vehicular UEs such as cars (running up to 140 km/h on a highway) [4] and trains (running up to 500 km/h for a high speed train) [5]. In the mmWave channel, a line-of-sight (LOS) path dominates over non-LOS (NLOS) paths, causing the channel to be less frequency selective (or alternatively speaking, the channel has a large coherence bandwidth), thereby alleviating the need for the short subcarrier spacing. Delay spread values are typically assumed to be in the order of 10 ns both for the mmWave-based high speed train [44] and V2X applications [4], in the 3GPP standardization. These delay spread assumptions can be verified through ray-tracing simulations [45] and measurements [19]. Then, the corresponding coherence bandwidth results in tens of MHz [46], leading to a conclusion that channel frequency selectivity is not a significant factor in the numerology design of the mmWave-based vehicular systems.

When it comes to the time-domain channel properties, it is apparent that the channel will have a short coherence time due to the high vehicle speeds. Moreover, the amount of Doppler shift/spread is also proportional to the carrier frequency. Assuming a UE speed of 500 km/h and a carrier frequency of 25 GHz, the maximum Doppler shift is 11.58 kHz, where the corresponding channel coherence time is 21.59 μs [46]. In this situation, link performance will be significantly degraded due to the Doppler-induced inter-carrier interference (ICI), unless the OFDM symbol duration is sufficiently short such that the channel variation is ignorable during the symbol duration.

Therefore, in order to satisfy the above frequency- and time-domain channel conditions, the subcarrier spacing of 180 kHz is selected. The corresponding OFDM symbol length is 5.56 μs excluding cyclic prefix (CP) or is 6.25 μs including CP. The fast Fourier transform (FFT) with 1024 points is employed, thereby resulting in a sampling rate of 184.32 MHz. The actually used number of subcarriers are 600, and the corresponding system bandwidth of each component carrier (CC) is 125 MHz. Several CCs (i.e., from 2 to 8) can be aggregated to support the total aggregated bandwidth of up to 1 GHz.

Fig. 2 shows the frame structure of the proposed vehicular communication system. Each radio frame is 10 ms long and consists of 5 subframes. Then, each subframe is 2 ms long and is divided into 8 slots. Since TDD is employed, each

TABLE 1. System parameters.

Parameter	Proposed system	LTE-A	5G NR
Carrier frequency	25.6 GHz	Below 6 GHz	Below and above 6 GHz
CC bandwidth	125 MHz	1.4-20 MHz	5-400 MHz
Number of CCs	2-8	1-5	1-16
Subcarrier spacing	180 kHz	15 kHz	15-240 kHz
FFT size	1024	Up to 2048	Up to 4096
Sampling rate	184.32 MHz	1.92-30.72 MHz	7.68-491.52 MHz
Number of used subcarriers	600	Up to 1200	Up to 3300
OFDM symbol length	5.56 μs	66.67 μs	4.17-66.67 μs
CP length	0.69 μs	4.69 μs	0.30-4.76 μs
Number of symbols per slot	40	7	14
Slot length	250 μs	500 μs	62.5-1000 μs

slot is either for a downlink, an uplink, or a special slot. The special slot consists of reduced downlink and uplink slots and a guard period between them, enabling to switch transmission from downlink to uplink, similar to LTE [47]. Three different downlink-uplink slot configurations are defined for different downlink-uplink ratios. Each slot is of length 250 μs and contains 40 OFDM symbols. In the frequency-domain, one resource block (RB) consists of 12 subcarriers. In the time-domain, the control region has a length of 2 symbols and is located at the starts of the downlink and special slots. The detailed system parameters including numerology and frame structure are summarized in Table 1, where the system parameters for the LTE-A and 5G NR are also provided for comparison.

Another important physical layer design consideration regarding high Doppler effect is the reference signal, which is used for estimating not only the highly time-varying channel coefficients but also the Doppler-induced frequency offset [48]. Regarding the time-varying channel estimation, time-domain reference signal density needs to be sufficiently high enough to avoid the channel estimation errors due to fast channel variation. We can find the minimum time interval T_p between the consecutive reference signals considering the Nyquist sampling theorem, i.e., $1/T_p \geq 2 f_D$, where f_D is the above-calculated maximum Doppler shift of 11.582 kHz. In the proposed system, the above condition is fully satisfied by selecting $T_p = 25$ μs, or equivalently 4 OFDM symbols, between the consecutive reference signal containing symbols. The determined reference signal pattern is lattice-type and supports up to 2 orthogonal antenna ports, as seen in Fig. 2. Regarding the frequency offset estimation, the proposed reference signal design allows the frequency offset estimation range to be $[-20, 20]$ kHz, which is sufficient for our high mobility requirement. The estimated frequency offset is then compensated by the automatic frequency control (AFC) unit in the time-domain.

In order to find whether the reference signal of the proposed system is suitable for supporting high Doppler scenarios, link-level performance evaluation results are provided. Fig. 3 shows the spectral efficiency of the proposed system as a function of signal-to-noise ratio (SNR) for different vehicle UE speeds of $\{100, 300, 500\}$ km/h. Single and dual-layer transmissions are assumed for the simulation. The speed of 100 km/h represents a car running on the highway. The speeds of 300 km/h and 500 km/h represent a high speed train. The system parameters given in Table 1 are used for the simulation. An adaptive modulation and channel coding scheme is employed where the modulation scheme is from QPSK to 64QAM and the code rate is from 0.117 to 0.889. For the channel coding schemes, turbo and convolutional coding schemes are employed for the data and control channels, respectively. It is seen that the spectral efficiency decreases with the vehicle speed. However, performance loss due to high speed is not significant until the speed of 300 km/h, and satisfactory spectral efficiency is still attainable even with the speed of 500 km/h. These results are actually the outcomes of our system design optimized for the high UE mobility scenario which is contrast to most existing cellular systems like LTE mainly targeting low-to-mid UE mobility UEs.

As a means of exploiting a multi-antenna scheme, antenna polarization is employed, which is quite useful in the mmWave-based vehicular scenario with limited scattering [49], [50]. Accordingly, a dual-polarized 2×2 MIMO scheme is employed, where the signals on the vertically polarized and horizontally polarized components are independently transmitted, as seen in Fig. 4. In a strong LOS channel, the depolarization between the vertically polarized and horizontally polarized components is minimized due to reduced reflection and scattering. Although there will be some remaining inter-polarization interference, these can be effectively mitigated using receiver signal processing techniques such as polarization filtering [51]. We support spatial multiplexing for enhancing data rate and spatial diversity for improving reliability. As already stated, in order to estimate MIMO channel coefficients at the receiver, the reference signals for the two orthogonal antenna ports are allocated in a lattice pattern (Fig. 2). In addition, considering high mobility, we employ an open-loop spatial multiplexing scheme rather than closed-loop techniques that are quite sensitive to the channel feedback delay [52].

B. HANDOVER SUPPORT FOR A LINEARLY DEPLOYED NETWORK

As a means of supporting mobility between neighboring cells, a handover procedure is required, which is of more importance in vehicular communication systems with high mobility

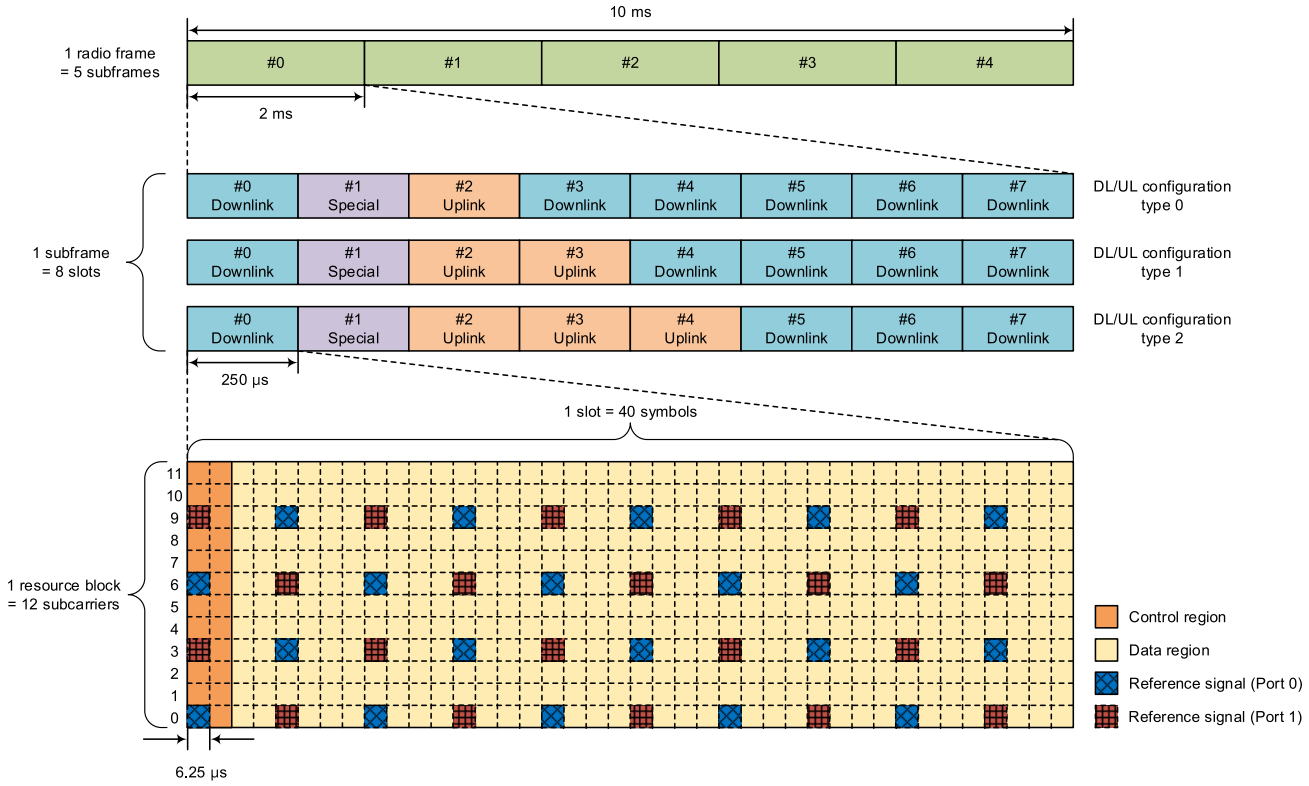

FIGURE 2. Frame structure of the proposed vehicular communication system.

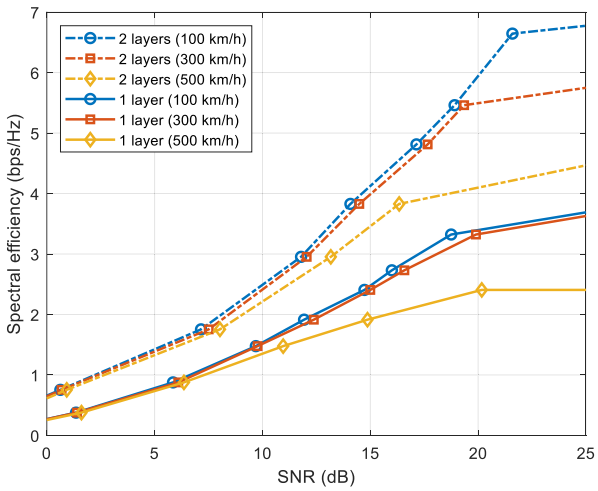

FIGURE 3. Spectral efficiency vs. SNR for different vehicle UE speeds.

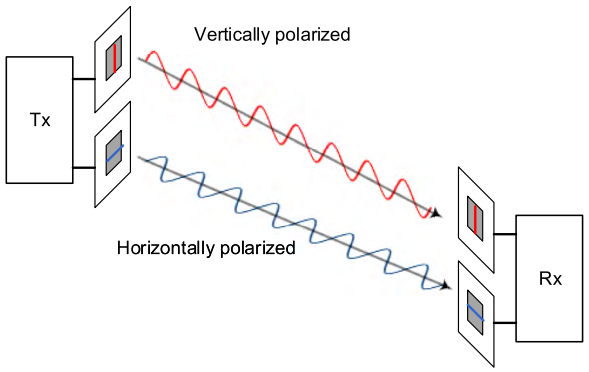

FIGURE 4. Dual-polarized MIMO scheme.

UEs. Conventional handover mechanisms are based on the received signal strength comparison, i.e., triggering handover if the received signal strength of the target RU exceeds that of the serving RU with a given margin offset [53]. These kinds of handover triggering schemes work well in traditional cellular networks where the received signal strengths from both the serving and target RUs vary smoothly.

However, in the vehicular system where the RUs are linearly deployed along the road or railway as seen in Fig. 1, there will be sudden variation in the received signal strength at the cell boundary. Fig. 5 shows the SNR distributions of the received signals from the serving and target RUs as a function of the UE location. It is assumed that each RU (located at 1000m and 2000m) produces a beam along the road or railway and the vehicle UE moves toward the RUs. We see that the received SNR gradually increases as the UE approaches the RU but abruptly decreases at the moment the UE passes by the RU, which is due to the fact that only

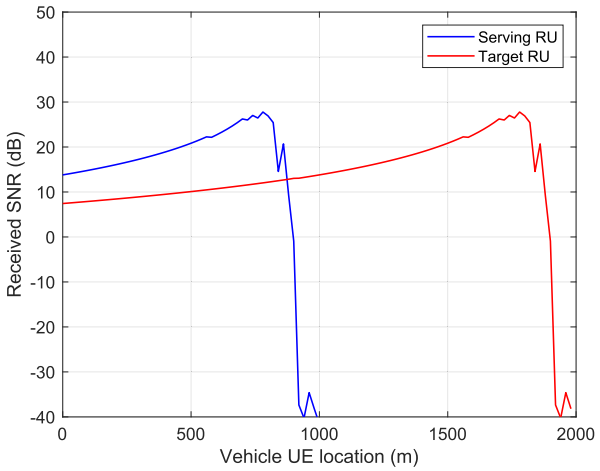

FIGURE 5. Received SNR along the vehicle UE location.

one-sided beam is generated from each RU. Consequently, it becomes very difficult to trigger handover because the received signal strength difference between the serving and target RUs are quite large. In other words, detecting the synchronization signal from the target RU (which is very weak) is quite challenging under the presence of such strong interference from the serving RU. The signal detection from the target RU will be possible after losing connection with the serving RU, leading to a large delay until the connection with the target RU is established. What is worse is that this handover event will be quite frequent due to higher vehicle speed. It will take only 7.2 seconds to travel 1 km for a high speed train running at 500 km/h.

The aforementioned handover difficulty regarding the synchronization to the target RU can be resolved by an improved carrier aggregation structure. We propose to alternate the locations of the synchronization signal block between the CCs, e.g., CC #0 and CC #1. At the same time, the time-frequency resources having the same location with that of the target cell are vacated, as seen in Fig. 6. By doing so, the detection of the synchronization signal from the target RU will be done without interference from the neighboring cells. Although the proposed scheme may slightly increase the overhead due to resource nulling, the handover failure rate will be significantly reduced.

IV. TESTBED IMPLEMENTATION AND VALIDATION

This section provides the details of testbed implementation of the proposed vehicular communication system including baseband modem, RF front-end, and antenna unit. In addition, the experimental validation through real-world field tests is presented.

A. BASEBAND MODEM IMPLEMENTATION

The functional structures of the baseband modem are depicted in Fig. 7 for the DU and in Fig. 8 for the vehicle UE, respectively. Both the DU and vehicle UE modems

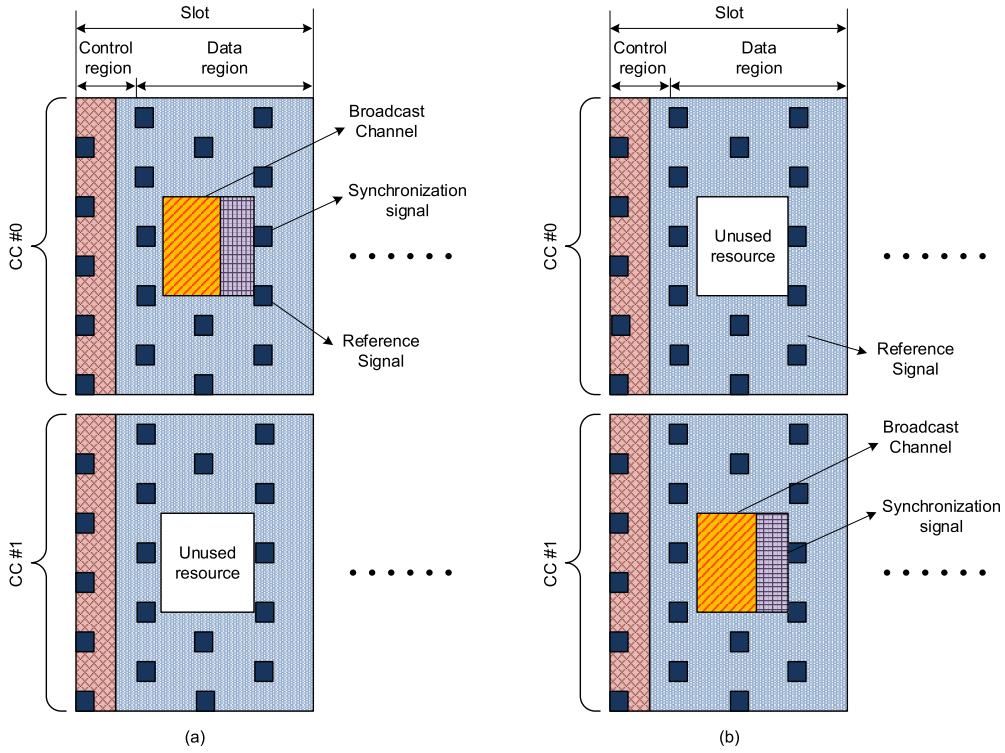

FIGURE 6. Synchronization signal switching and resource nulling scheme: a) Serving cell; b) Target cell.

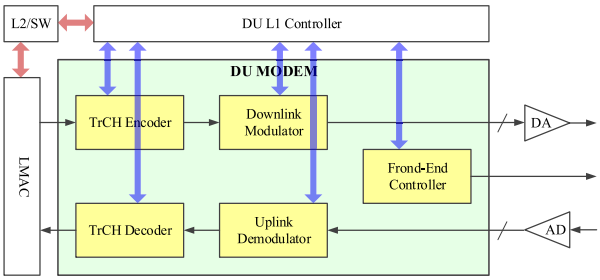

FIGURE 7. DU baseband modem structure.

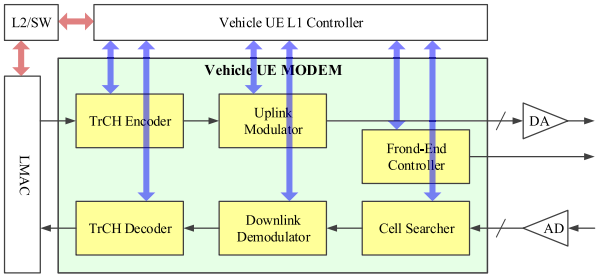

FIGURE 8. UE baseband modem structure.

commonly contain transport channel (TrCH) encoder and decoder, modulator and demodulator, and front-end controller. Turbo encoding/decoding and cyclic-buffer rate matching/recovery functionalities are implemented at the TrCH encoder and decoder. A front-end controller is responsible for controlling and monitoring the operation of the RF front-end. In the vehicle UE modem, a cell searcher is implemented, which acquires time and frequency synchronization, frame timing, and cell identity. For both DU and vehicle UE modems, interfaces to the corresponding L1 controller are configured.

Based on the above baseband modem structure, we implemented the DU baseband modem as seen in Fig. 9. Main modem functionalities such as modulation/demodulation modules are implemented using 5 field-programmable gate array (FPGA) chips (Xilinx Kintex7 UltraScale XCKU115). More specifically, 1 FPGA is used for the processing of the analog/digital interface, PCIe interface, and DDR memory interface. The rest 4 FPGAs are used for the data processing, each of which is responsible for 2 CCs. Channel encoding and decoding are processed using dedicated chips. Analog-to-digital (AD) and digital-to-analog (DA) converters operating with frequency of 1843.2 MHz are used. TI ADC32RF45 is used for AD converter which supports 4 Gsps. TI DAC38RF89 is used for DA converter which supports 8.4 Gsps. Micro controller unit (MCU) chip (STM32F746NGH6) is employed for L1 control. The PCIe interface is used between L2/L3 and DU. The RoF module is responsible for connecting between DU and RUs.

B. RF FRONT-END IMPLEMENTATION

The interior of the RU module is depicted in Fig. 10. There are 2 TX and 2 RX RF paths in the RU module. A power supply, a local oscillator, and an RoF interface module are also included. The RU module is assembled so as to satisfy the

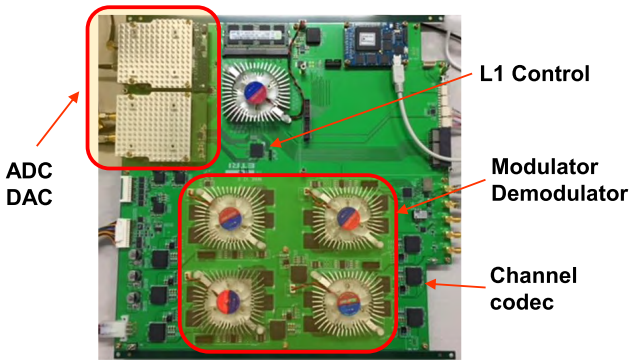

FIGURE 9. DU baseband modem implementation.

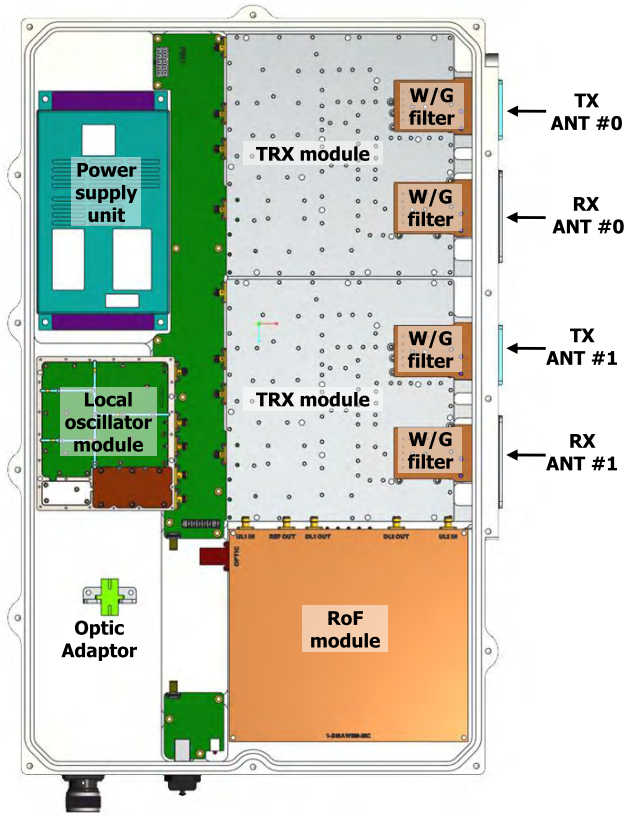

FIGURE 10. RU module implementation.

water protection IP65 and a certain vibration resistance levels. The RU module has an LED in its exterior which enables to display an alarm event. A debugging port for monitoring and controlling is also provided. Thermal analysis is carried out during the heat sink design and package size optimization.

Slotted waveguide array antennas are employed in order to maximize the radiation efficiency with limited dimension as seen in Fig. 11. Each TX array antenna has 4×4 radiating elements with an array gain of 19 dBi. Each RX array antenna has 6×6 radiating elements with an array gain of 22 dBi. The TX array antenna should keep the regulatory output power in terms of equivalent isotropic radiated power (EIRP), i.e., the sum of the maximum output power and the array gain

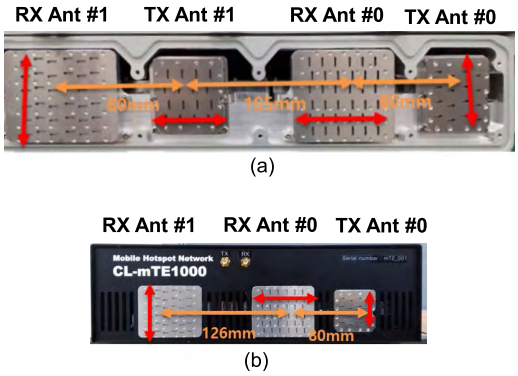

FIGURE 11. Antenna implementation (Double arrows represent the direction of antenna polarization); a) RU antenna configuration; b) vehicle UE antenna configuration.

should be lower than 36 dBm. Dual-polarized transmission and reception is supported at the RU TX and the vehicle UE RX respectively, allowing 2 × 2 dual-polarized MIMO transmission in the downlink.

C. FIELD TRIAL

We describe the field trial results performed in actual subway tunnel and urban road environments.

1) SUBWAY TUNNEL ENVIRONMENT

The proposed vehicular communication system was tested in a running subway train of Seoul subway line 8. Fig. 12 shows a subway map of Seoul metropolitan area in Korea and a segment of the subway path in which the test was carried out. There are three stations, namely Jamsil, Seokchon, and Songpa stations from left to right in the testing path. Inside the subway tunnel, each RU was deployed along the tunnel walls as seen in Fig. 12 (bottom-left corner). The height of each RU is around 2.5m, which is similar to that of the vehicle UE for consistent beam alignment regardless of the train location. Four RUs were installed between Jamsil station and Seokchon station to cover the curved path. One RU was installed near the Songpa station which can cover the entire straight path. The locations of these five RUs were determined after a dedicated wave propagation test.

Each vehicle UE was mounted in the subway driver's cab, just behind the subway's windshield. As the subway moves through the route, the vehicle UE receives and transmits signals from/to the nearest RU. It also carries out the handover operation when crossing each RU location (or equivalently cell boundary). Fig. 12 (bottom-right corner) shows the captured performance monitoring display that includes downlink (green curve) and uplink (blue curve) data throughput. It shows around 1.25 Gbps of downlink data rate is achieved with an aggregated bandwidth of 500 MHz for most of the time.

2) URBAN ROAD ENVIRONMENT

The test for the urban road environment was carried out in Gangneung, Korea. As seen in Fig. 13, RUs are deployed along the Yulgok street so that each RU forms a beam along the road. The height of each RU is around a few tens of

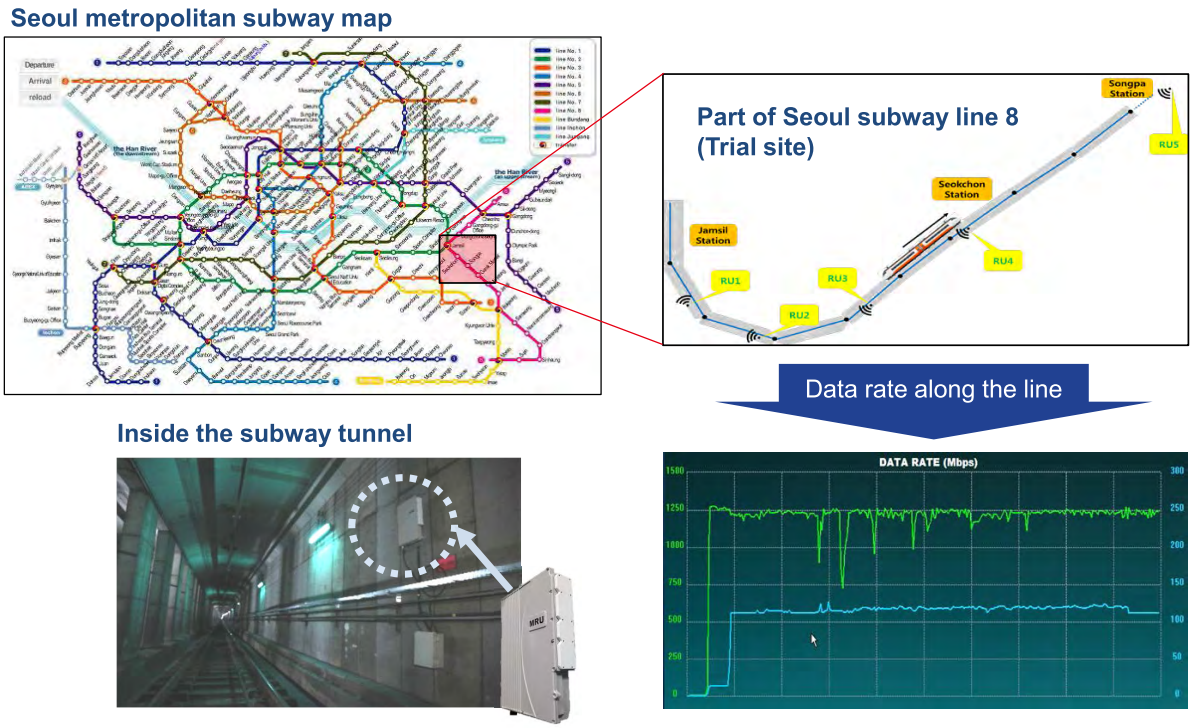

FIGURE 12. Subway tunnel test environment and results.

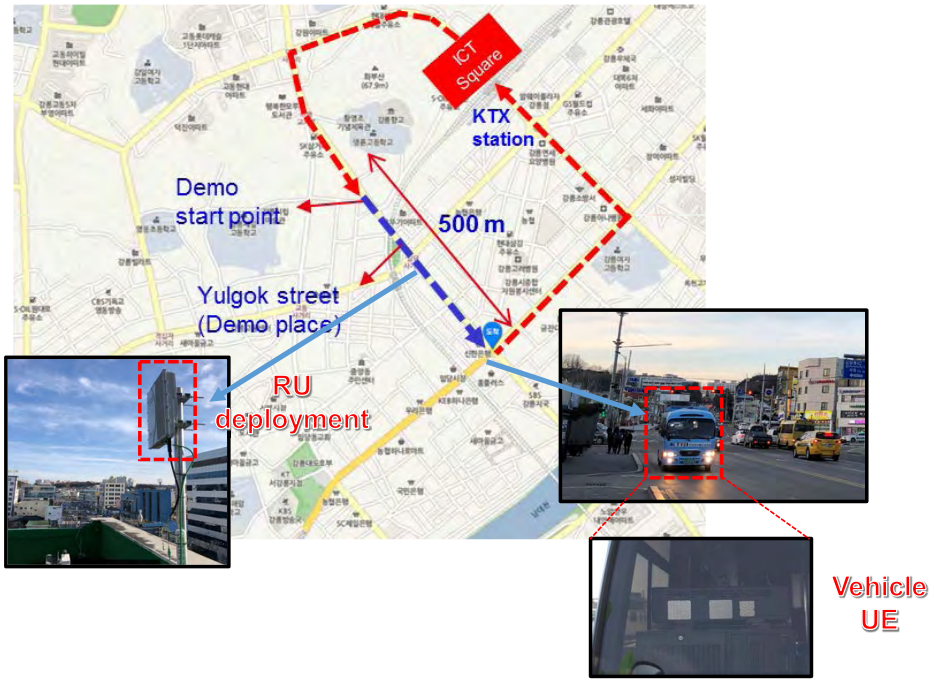

FIGURE 13. Urban road test environment and results.

Apply a display filter ... <Ctrl-/>

No.	Time	Source	Destination	Protocol	Lengt	Info
1	*REF*	192.168.254.101	192.168.100.64	ICMP	100	Echo (ping) request id=0x366c, seq=1/256, ttl=64 (no respor
2	0.002184	192.168.254.101	192.168.100.64	ICMP	100	Echo (ping) request id=0x366c, seq=1/256, ttl=64 (no respor
3	1.007588				100	<Ignored>
4	*REF*	192.168.254.101	192.168.100.64	ICMP	100	Echo (ping) request id=0x366c, seq=3/768, ttl=64 (no respor
5	0.002597	192.168.254.101	192.168.100.64	ICMP	100	Echo (ping) request id=0x366c, seq=3/768, ttl=64 (no respor
6	1.007999				100	<Ignored>
7	2.016003				100	<Ignored>
8	*REF*	192.168.254.101	192.168.100.64	ICMP	100	Echo (ping) request id=0x366c, seq=6/1536, ttl=64 (no respo
9	0.002556	192.168.254.101	192.168.100.64	ICMP	100	Echo (ping) request id=0x366c, seq=6/1536, ttl=64 (no respo
10	1.007984				100	<Ignored>
11	*REF*	192.168.254.101	192.168.100.64	ICMP	100	Echo (ping) request id=0x366c, seq=8/2048, ttl=64 (no respo
12	0.002546	192.168.254.101	192.168.100.64	ICMP	100	Echo (ping) request id=0x366c, seq=8/2048, ttl=64 (no respo

FIGURE 14. Measurement of user plane latency.

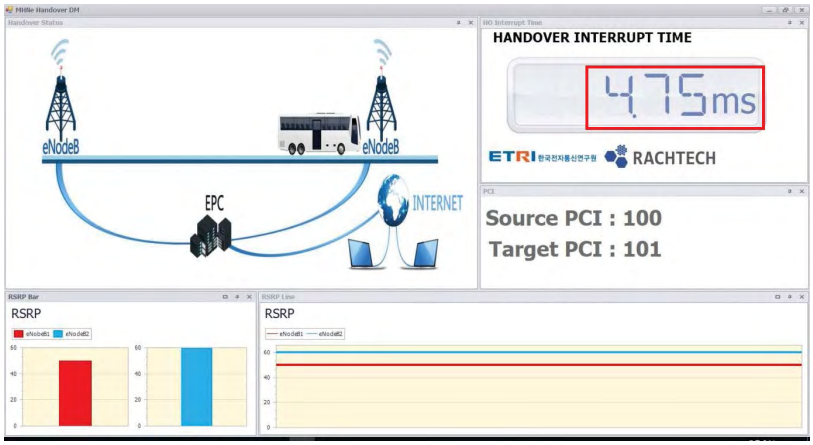

FIGURE 15. Measurement of handover interruption time.

meters. The main reason of having higher RU height than that in the subway tunnel scenario is to minimize the potential blockage due to vehicles which may obstruct the link between the RU and the vehicle UE. Although the vehicle UE close to the RU may experience weaker signal due to the elevated RU, it can be overcome by the proper antenna tilting and handover triggering operation. The distance between the RUs is 500m. The vehicle UEs were deployed at the front of a bus.

During the link performance test, the data rate was 5 Gbps in maximum and 2-4 Gbps on average with an aggregated bandwidth of 1 GHz under the 2-layer spatial multiplexing transmission mode.

3) LATENCY AND HANDOVER TEST RESULTS

We also evaluated some key performance metrics regarding latency and handover. We measured user-plane latency, which is defined as the time during which an application layer packet is successfully delivered between the layer 2/3 service data units (SDUs) of the base station and device [5]. The user plane latency was measured by 2.546 ms after a ping test, as seen in Fig. 14, which is much less than the 5G requirement of 4 ms for eMBB. Regarding the handover performance, we measured handover interruption time that means the shortest time duration during which a mobile device cannot exchange user plane packets due to mobility procedure (i.e., handover) [5]. The handover interruption time of the proposed system was measured by 4.75 ms during the bus trial as seen in Fig. 15.

V. CONCLUSION AND FUTURE DIRECTION

In this paper, we presented a promising design for realizing multi-Gbps vehicular communication focusing on the high mobility and mmWave frequency bands. Based on the relaying network architecture, we proposed a system design involved in a rich set of design elements including numerology, frame structure, reference signal, multi-antenna scheme, and handover. The proposed system was implemented into a real testbed consisting of baseband modem, RF front-end, and antenna units. The developed testbed was validated through real-world field tests both in subway tunnel and urban road environments.

The work done in this paper can be extended to other vehicular communication scenarios such as V2V communications involving sidelink transmissions, introducing several further technical challenges including dual mobility, synchronization, and resource allocation. Another future topics may include the integration of the in-vehicle access link and out-of-vehicle backhaul link, which can further improve the quality-of-service (QoS) of the users inside the vehicles.

REFERENCES

[1] *Minimum Requirements Related to Technical Performance for IMT-2020 Radio Interface(s)*, document ITU-R M.2410-0, Nov. 2017.

[2] J. Wu and P. Fan, "A survey on high mobility wireless communications: Challenges, opportunities and solutions," *IEEE Access*, vol. 4, pp. 450–476, 2016.

[3] *NGMN 5G White Paper, v1.0*, NGMN, Frankfurt, Germany, Feb. 2015.

[4] *Study on Evaluation Methodology of New Vehicle-to-Everything V2X Use Cases for LTE and NR*, document 3GPP TR 37.885, v. 15.0.0, Jun. 2018.

[5] *Study on Scenarios and Requirements for Next Generation Access Technologies*, document 3GPP TR 38.913, v. 14.3.0, Jun. 2017.

[6] S. Herbert, I. Wassell, T.-H. Loh, and J. Rigelsford, "Characterizing the spectral properties and time variation of the in-vehicle wireless communication channel," *IEEE Trans. Commun.*, vol. 62, no. 7, pp. 2390–2399, Jul. 2014.

[7] T. S. Rappaport *et al.*, "Millimeter wave mobile communications for 5G cellular: It will work!" *IEEE Access*, vol. 1, pp. 335–345, May 2013.

[8] J. G. Andrews, T. Bai, M. N. Kulkarni, A. Alkhateeb, A. K. Gupta, and R. W. Heath, Jr., "Modeling and analyzing millimeter wave cellular systems," *IEEE Trans. Commun.*, vol. 65, no. 1, pp. 403–430, Jan. 2017.

[9] R. He *et al.*, "High-speed railway communications: From GSM-R to LTE-R," *IEEE Veh. Technol. Mag.*, vol. 11, no. 3, pp. 49–58, Sep. 2016.

[10] S. Chen *et al.*, "Vehicle-to-everything (V2X) services supported by LTE-based systems and 5G," *IEEE Commun. Standards Mag.*, vol. 1, no. 2, pp. 70–76, Jun. 2017.

[11] L. Tian, J. Li, Y. Huang, J. Shi, and J. Zhou, "Seamless dual-link handover scheme in broadband wireless communication systems for high-speed rail," *IEEE J. Sel. Areas Commun.*, vol. 30, no. 4, pp. 708–718, May 2012.

[12] M.-S. Pan, T.-M. Lin, and W.-T. Chen, "An enhanced handover scheme for mobile relays in LTE-A high-speed rail networks," *IEEE Trans. Veh. Technol.*, vol. 64, no. 2, pp. 743–756, Feb. 2015.

[13] C. X. Wang, A. Ghazal, B. Ai, P. Fan, and Y. Liu, "Channel measurements and models for high-speed train communication systems: A survey," *IEEE Commun. Surveys Tuts.*, vol. 18, no. 2, pp. 974–987, 2nd Quart., 2016.

[14] V. Va, J. Choi, and R. W. Heath, Jr., "The impact of beamwidth on temporal channel variation in vehicular channels and its implications," *IEEE Trans. Veh. Technol.*, vol. 66, no. 6, pp. 5014–5029, Jun. 2017.

[15] K. Guan *et al.*, "Towards realistic high-speed train channels at 5G millimeter-wave band—Part I: Paradigm, significance analysis, and scenario reconstruction," *IEEE Trans. Veh. Technol.*, vol. 67, no. 10, pp. 9112–9128, Oct. 2018.

[16] D. He *et al.*, "Influence of typical railway objects in a mmWave propagation channel," *IEEE Trans. Veh. Technol.*, vol. 67, no. 4, pp. 2880–2892, Apr. 2018.

[17] B. Antonescu, M. T. Moayyed, and S. Basagni, "mmWave channel propagation modeling for V2X communication systems," in *Proc. IEEE Int. Symp. Pers. Indoor Mobile Radio Commun. (PIMRC)*, Oct. 2017, pp. 1–6.

[18] J.-J. Park, J. Lee, K.-W. Kim, K.-C. Lee, and M.-D. Kim, "Vehicle antenna position dependent path loss for millimeter-wave V2V communication," in *Proc. Global Symp. Millim. Waves (GSMM)*, May 2018, pp. 1–3.

[19] M. G. Sánchez, M. P. Táboas, and E. L. Cid, "Millimeter wave radio channel characterization for 5G vehicle-to-vehicle communications," *Measurement*, vol. 95, pp. 223–229, Jan. 2017.

[20] I. Rodriguez *et al.*, "Measurement-based evaluation of the impact of large vehicle shadowing on V2X communications," in *Proc. Eur. Wireless (EW)*, May 2016, pp. 1–8.

[21] Z. Dong, P. Fan, R. Q. Hu, J. Gunther, and X. Lei, "On the spectral efficiency of rate and subcarrier bandwidth adaptive OFDM systems over very fast fading channels," *IEEE Trans. Veh. Technol.*, vol. 65, no. 8, pp. 6038–6050, Aug. 2016.

[22] F. Hasegawa *et al.*, "3GPP standardization activities in relay based 5G high speed train scenarios for the SHF band," in *Proc. IEEE Conf. Standards Commun. Netw. (CSCN)*, Sep. 2016, pp. 126–131.

[23] H. Song, X. Fang, and Y. Fang, "Millimeter-wave network architectures for future high-speed railway communications: Challenges and solutions," *IEEE Wireless Commun.*, vol. 23, no. 6, pp. 114–122, Dec. 2016.

[24] N. Sun and J. Wu, "Maximizing spectral efficiency for high mobility systems with imperfect channel state information," *IEEE Trans. Wireless Commun.*, vol. 13, no. 3, pp. 1462–1470, Mar. 2014.

[25] G. Noh, B. Hui, J. Kim, H. S. Chung, and I. Kim, "DMRS design and evaluation for 3GPP 5G new radio in a high speed train scenario," in *Proc. IEEE Global Telecommun. Conf. (GLOBECOM)*, Dec. 2017, pp. 1–6.

[26] N. Garcia, H. Wymeersch, E. G. Ström, and D. Slock, "Location-aided mm-wave channel estimation for vehicular communication," in *Proc. IEEE Int. Workshop Signal Process. Adv. Wireless Commun. (SPAWC)*, Jul. 2016, pp. 1–5.

[27] C. Zhang, G. Wang, M. Jia, R. He, L. Zhou, and B. Ai, "Doppler shift estimation for millimeter-wave communication systems on high-speed railways," *IEEE Access*, to be published.

[28] S. N. Choi, D. You, I. Kim, and D. J. Kim, "Uplink design of millimeter-wave mobile communication systems for high-speed trains," in *Proc. IEEE Veh. Technol. Conf. (VTC Spring)*, May 2014, pp. 1–5.

[29] Y. Cui, X. Fang, and L. Yan, "Hybrid spatial modulation beamforming for mmWave railway communication systems," *IEEE Trans. Veh. Technol.*, vol. 65, no. 12, pp. 9597–9606, Dec. 2016.

[30] I. Mavromatis, A. Tassi, R. J. Piechocki, and A. Nix, "mmWave system for future ITS: A MAC-layer approach for V2X beam steering," in *Proc. IEEE Veh. Technol. Conf. (VTC Fall)*, Sep. 2017, pp. 1–6.

[31] M. Polese, M. Giordani, M. Mezzavilla, S. Rangan, and M. Zorzi, "Improved handover through dual connectivity in 5G mmWave mobile networks," *IEEE J. Sel. Areas Commun.*, vol. 35, no. 9, pp. 2069–2084, Sep. 2017.
[32] Z. Liu and P. Fan, "An effective handover scheme based on antenna selection in ground–train distributed antenna systems," *IEEE Trans. Veh. Technol.*, vol. 63, no. 7, pp. 3342–3350, Sep. 2014.
[33] J. Wang, H. Zhu, and N. J. Gomes, "Distributed antenna systems for mobile communications in high speed trains," *IEEE J. Sel. Areas Commun.*, vol. 30, no. 4, pp. 675–683, May 2012.
[34] S. Umeda, A. Okazaki, H. Nishimoto, K. Tsukamoto, K. Yamaguchi, and A. Okamura, "Cell structure for high-speed land-mobile communications," in *Proc. IEEE Veh. Technol. Conf. (VTC Fall)*, Sep. 2015, pp. 1–5.
[35] W. Luo, R. Zhang, and X. Fang, "A CoMP soft handover scheme for LTE systems in high speed railway," *EURASIP J. Wireless Commun. Netw.*, vol. 2012, Jun. 2012.
[36] F. Hasegawa *et al.*, "High-speed train communications standardization in 3GPP 5G NR," *IEEE Commun. Standards Mag.*, vol. 2, no. 1, pp. 44–52, Mar. 2018.
[37] M. Boban, K. Manolakis, M. Ibrahim, S. Bazzi, and W. Xu, "Design aspects for 5G V2X physical layer," in *Proc. IEEE Conf. Standards Commun. Netw. (CSCN)*, Oct./Nov. 2016, pp. 1–7.
[38] G. Noh, J. Kim, H. S. Chung, B. Hui, Y.-M. Choi, and I. Kim, "mmWave-based mobile backhaul transceiver for high speed train communication systems," in *Proc. IEEE Global Commun. Conf. Workshops (GLOBECOM Workshops)*, Dec. 2017, pp. 1–5.
[39] D.-S. Cho, J. Kim, and I. Kim, "Outdoor demonstration of 5Gbps MHN enhanced system," in *Proc. Int. Conf. Ubiquitous Future Netw. (ICUFN)*, Jul. 2018, pp. 886–890.
[40] M. G. Larrode, A. M. J. Koonen, J. J. V. Olmos, and A. Ng'Oma, "Bidirectional radio-over-fiber link employing optical frequency multiplication," *IEEE Photon. Technol. Lett.*, vol. 18, no. 1, pp. 241–243, Jan. 1, 2006.
[41] D. Visani, G. Tartarini, L. Tarlazzi, and P. Faccin, "Transmission of UMTS and WIMAX signals over cost-effective radio over fiber systems," *IEEE Microw. Wireless Compon. Lett.*, vol. 19, no. 12, pp. 831–833, Dec. 2009.
[42] W. Lee and D.-H. Cho, "Group handover scheme using adjusted delay for multi-access networks," in *Proc. IEEE Int. Conf. Commun. (ICC)*, May 2010, pp. 1–5.
[43] M. Cudak *et al.*, "Moving towards mmWave-based beyond-4G (B-4G) technology," in *Proc. IEEE Veh. Technol. Conf. (VTC Spring)*, Jun. 2013, pp. 1–5.
[44] *Study on New Radio Access Technology: Physical Layer Aspects*, document 3GPP TR 38.802, v. 14.1.0, Jun. 2017.
[45] K. Guan *et al.*, "Scenario modules and ray-tracing simulations of millimeter wave and terahertz channels for smart rail mobility," in *Proc. Eur. Conf. Antennas Propag. (EUCAP)*, Mar. 2017, pp. 113–117.
[46] D. Tse and P. Viswanath, *Fundamentals of Wireless Communication*. Cambridge, U.K.: Cambridge Univ. Press, 2005.
[47] E. Dahlman, S. Parkvall, and J. Skold, *4G, LTE-Advanced Pro and the Road to 5G*. London, U.K.: Academic, 2016.
[48] H. Minn, V. K. Bhargava, and K. B. Letaief, "A robust timing and frequency synchronization for OFDM systems," *IEEE Trans. Wireless Commun.*, vol. 2, no. 4, pp. 822–839, Jul. 2003.
[49] W. Hong, K.-H. Baek, Y. Lee, Y. Kim, and S.-T. Ko, "Study and prototyping of practically large-scale mmWave antenna systems for 5G cellular devices," *IEEE Commun. Mag.*, vol. 52, no. 9, pp. 63–69, Sep. 2014.
[50] O. Jo, J.-J. Kim, J. Yoon, D. Choi, and W. Hong, "Exploitation of dual-polarization diversity for 5G millimeter-wave MIMO beamforming systems," *IEEE Trans. Antennas Propag.*, vol. 65, no. 12, pp. 6646–6655, Dec. 2017.
[51] S.-C. Kwon and G. L. Stuber, "Polarization division multiple access on NLoS wide-band wireless fading channels," *IEEE Trans. Wireless Commun.*, vol. 13, no. 7, pp. 3726–3737, Jul. 2014.
[52] Q. Li *et al.*, "MIMO techniques in WiMAX and LTE: A feature overview," *IEEE Commun. Mag.*, vol. 48, no. 5, pp. 86–92, May 2010.
[53] H.-S. Park, Y. Lee, T.-J. Kim, B.-C. Kim, and J.-Y. Lee, "Handover mechanism in NR for ultra-reliable low-latency communications," *IEEE Netw.*, vol. 32, no. 2, pp. 41–47, Mar./Apr. 2018.

GOSAN NOH (M'12) received the B.S. and Ph.D. degrees in electrical and electronic engineering from Yonsei University, Seoul, South Korea, in 2007 and 2012, respectively.

From 2012 to 2013, he was a Postdoctoral Researcher with the School of Electrical and Electronic Engineering, Yonsei University. Since 2013, he has been with the Electronics and Telecommunications Research Institute (ETRI), Daejeon, South Korea, where he is currently a Senior Researcher. He has contributed to several areas of telecommunications, including cognitive radio, spectrum sharing, millimeter-wave transmission, and high mobility applications. He has also been involved in the 3GPP fifth-generation new radio standardization as the ETRI's Delegate of the 3GPP RAN1 Working Group, since 2016. He has published 35+ scientific papers in journals and conferences.

JUNHYEONG KIM received the B.S. degree from the Department of Electronic Engineering, Tsinghua University, Beijing, China, in 2008, and the M.S. degree from the Department of Electrical Engineering, Korea Advanced Institute of Science and Technology (KAIST), Daejeon, South Korea, in 2011. He is currently pursuing the Ph.D. degree with the School of Electrical Engineering, KAIST.

Since 2012, he has been with the Electronics and Telecommunications Research Institute. His main research interests include millimeter-wave communications, multiple-input-multiple-output, cooperative communications, and handover.

HEESANG CHUNG received the bachelor's degree in physics from KAIST, South Korea, in 1993, and the Ph.D. degree in physics from Chungnam National University, South Korea, in 1999.

He had been involved in research projects on optical communications, from 1999 to 2005. He moved to the Wireless Communications Department, Electronics and Telecommunications Research Institute (ETRI), South Korea, in 2005. He had been involved in research projects on long-term evolution (LTE) and LTE Advanced, from 2006 to 2010. Since 1999, he has been with ETRI. His recent research interests include fifth-generation and millimeter-wave-based mobile communications, including mobile wireless backhauls for public transportation.

ILGYU KIM received the B.S. and M.S. degrees in electronic engineering from The University of Seoul, Seoul, South Korea, in 1993 and 1995, respectively, and the Ph.D. degree in information communications engineering from the Korea Advanced Institute of Science and Technology, Daejeon, South Korea, in 2009.

Since 2000, he has been with the Electronics and Telecommunications Research Institute, where he has been involved in the development of WCDMA, long-term evolution, and MHN systems. Since 2012, he has been the Leader of the Mobile Wireless Backhaul Research Section. His main research interests include millimeter-wave communications and fifth-generation mobile communications.